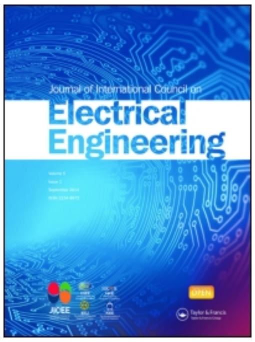

Journal of International Council on Electrical Engineering

ISSN: (Print) 2234-8972 (Online) Journal homepage: https://www.tandfonline.com/loi/tjee20

Analysis and optimization of frequency control in isolated microgrid with double-fed induction-generators based wind turbine

Khosro Khani & Ghazanfar Shahgholian

To cite this article: Khosro Khani & Ghazanfar Shahgholian (2019) Analysis and optimization of frequency control in isolated microgrid with double-fed induction-generators based wind turbine, Journal of International Council on Electrical Engineering, 9:1, 24-37, DOI: 10.1080/22348972.2018.1564547

To link to this article: https://doi.org/10.1080/22348972.2018.1564547

Published online: 13 Feb 2019.

JOURNAL OF INTERNATIONAL COUNCIL ON ELECTRICAL ENGINEERING
2019, VOL. 9, NO. 1, 24–37
https://doi.org/10.1080/22348972.2018.1564547

ARTICLE

OPEN ACCESS Check for updates

Analysis and optimization of frequency control in isolated microgrid with double-fed induction-generators based wind turbine

Khosro Khani[a] and Ghazanfar Shahgholian[b]

[a]Smart Microgrid Research Center, Najafabad Branch, Islamic Azad University, Najafabad, Iran; [b]Department of Electrical Engineering, Najafabad Branch, Islamic Azad University, Najafabad, Iran

ABSTRACT

In this paper the role of wind energy conversion systems (WECS) was investigated, In particular, variable speed wind turbines (VSWT) based on double-fed induction-generator (DFIG) in control and the optimization frequency with different wind penetration in the isolated system including Traditional Thermal and Non-thermal units have been investigated too. DFIG is capable of providing power at different mechanical speeds and reducing the Instantaneous speed, thus the release of stored mechanical energy; it is able to support traditional units of frequency tuning system. By achieving this through setting the desired speed, controlling DFIG at different levels of wind penetration is possible. This technique utilizes the particle swarm optimization (PSO) algorithm. The simulation results have been compared to the integral of squared error (ISE). The optimal penetration of WECSs by considering changing parameters in the microgrid (MG) frequency is investigated. The presence of wind turbines has been shown to improve the oscillation frequency and In particular the penetration rate of the wind turbine in the MG. The best frequency control will be achieved. To achieve the computing purposes, use of intelligent algorithms is much better than the methods trial and error methods.

ARTICLE HISTORY
Received 2 February 2018
Accepted 28 December 2018

KEYWORDS
Control frequency; wind energy conversion systems; micro grid; integral of squared error; particle swarm optimization

1. Introduction

Nowadays reduced economic dependency on fossil fuels due to ever-increasing energy demands, limitation of fossil fuel resources, environmental pollution caused by fossil fuels, global warming, greenhouse effects, and many other factors have led the world to focus on renewable energies [1,2]. Wind power, among wide variety of renewable energies, is considered as one of the optimistic technologies [3,4]. Using wind energy for electric power production is growing because of robust infrastructures, technological advancement, and low operating cost [5,6]. With the increased wind energy penetration in MGs, new challenges have been appeared with regard to the MG performance such as stability, balance, security, commercial programming and design of MG. Wind power has an intermittent nature, thus, large accumulation of wind power in a MG can significantly influence the design, performance and control of MG. This, in turn, leads to reduced effective frequency drop when DFIG controller is optimally tuned by ISE method [7]. Several efforts have been reported on DFIG-based wind turbines in order to demonstrate independent control of active and reactive power [8,9]. Accordingly, the use of DFIG based wind turbines are of great advantage for utilities compared to the fixed speed turbines [10,11]. A detail dynamic model and a control of a DFIG-based variable-speed wind-turbine grid-connected system in the dq-synchronous reference frame is presented in [12]. A detailed algorithm for the effect of wind farm connection to a certain power system on the system frequency response is presented in [13], which detailed analysis for the system frequency response in case of normal and fault operations were conducted. Authors of [14] presented the concept of kinetic energy release of DFIG-based wind turbines while power system frequency is reduced in order to prevent system inertia reduction. A control scheme of a grid-connected DFIG wind turbine with series grid-side converter to improve the control and operation performance of DFIG system during network unbalance is proposed in [15]. In [16], it was revealed that if wind turbines do not reduce the inertia at the time of light-load, system robustness will be greatly endangered. In other words, frequency drop of system can be remarkably improved if wind turbines contribute in system

CONTACT Ghazanfar Shahgholian shahgholian@iaun.ac.ir Department of Electrical Engineering, Najafabad Branch, Islamic Azad University, Najafabad, Iran

inertia support. In [17], schematic control for effective participation of DFIG-based wind turbines in adjustment of system frequency was proposed. Many researchers concluded that VSWTs have the capability of controlling initial frequency and inertia by employing supplemental control loops. To do this, the kinetic energy stored in hidden inertia of turbine blades is utilized [18]. In [19,20], frequency control of one and/or two-area of the system was examined with a combination of wind turbines, thermal and non-thermal turbines as well as hydrothermal turbines by employing ISE method, genetic algorithm (GA), fuzzy control, and frequency drop characteristic. DFIG based wind turbine with separate electrical power systems and mechanical rotor frequency, capable to produce power with various mechanical speeds. There is also the rotational inertia of the turbine blades and ability to reduce the

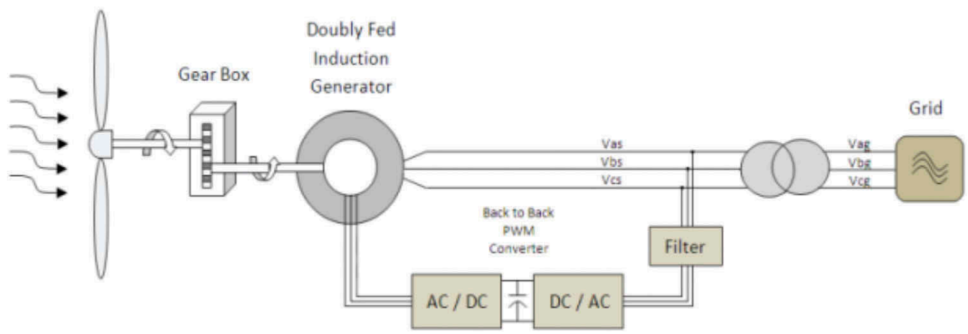

Figure 1. Double-fed induction-generator based wind turbine.

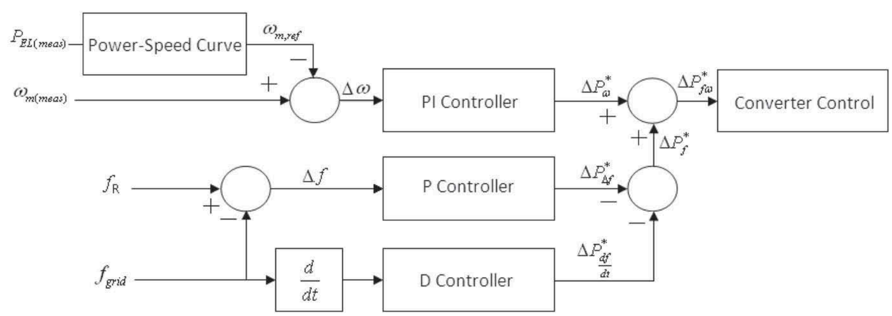

(a) Inertial emulation control

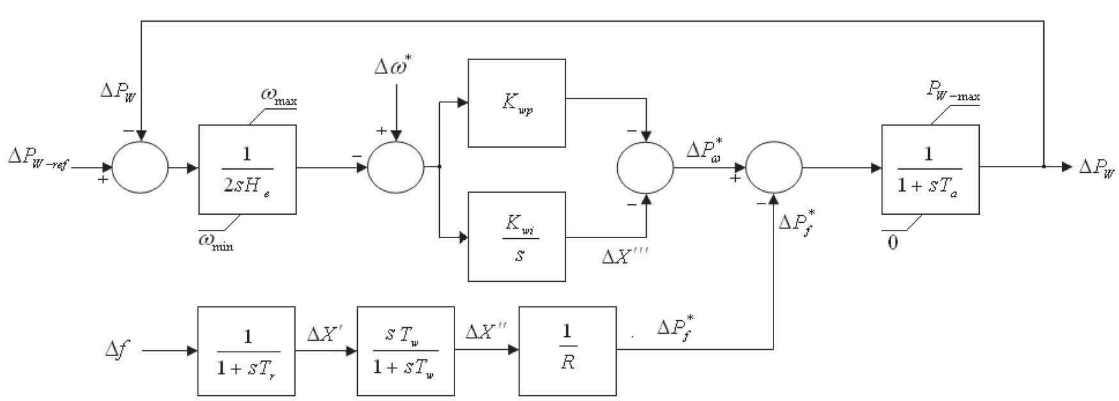

(b) Control based on frequency change

Figure 2. Double-fed induction-generator based wind turbines controllers [23]. (a) Inertial emulation control. (b) Control based on frequency change.

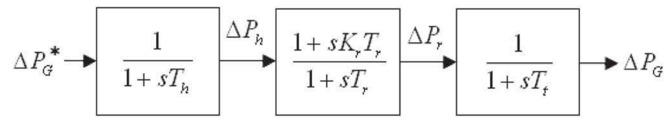

(a) With reheat

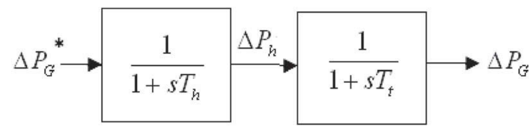

(b) Without reheat

Figure 3. Dynamic model of wind turbine. (a) With reheat. (b) Without reheat.

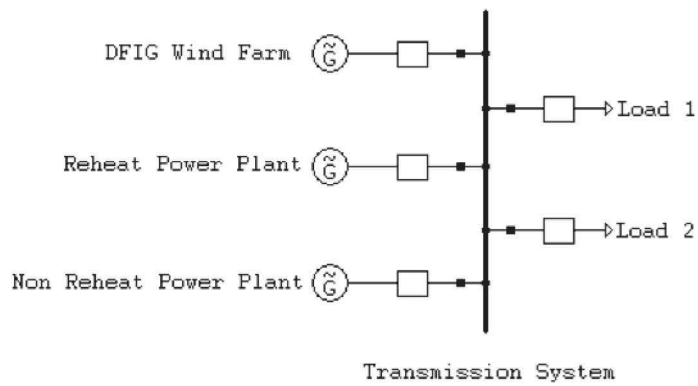

(a) Transmission power grid

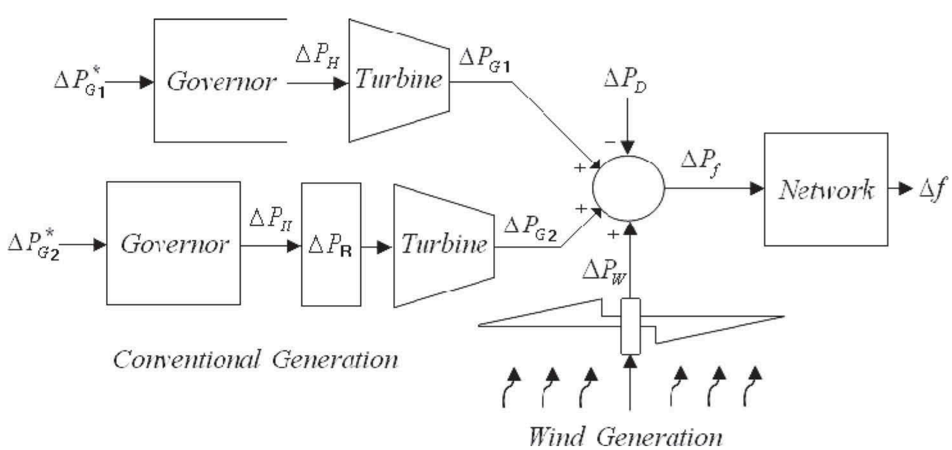

(b) Dynamic configuration of microgrid

Figure 4. Dynamic model of frequency control. (a) Transmission power grid. (b) Dynamic configuration of microgrid.

instantaneous speed and release of stored mechanical energy. By this system supporting the conventional generators for frequency adjustment is possible. Most articles focus on the wind turbine on MG and the impact of increased penetration of wind energy in conversion systems in small networks has not been studied [21,22].

In this paper, the role of DFIG based wind turbines, in control and tune of frequency were considered and various wind power penetration in a MG compromising of conventional generators also were studied. Setting the desired DFIGs speed controllers by using PSO algorithm for various wind power penetration levels has been done and the results were compared to the ISE in references [23]. Furthermore, the impact of increasing the wind power penetration level on frequency variation caused by load changes in the studied MG also is investigated. Simulation results revealed that the proposed technique could improve the quality of frequency variation and conventional generators power variation imposed by overload and perturbations into MG. This improvement was obtained in any penetration level of wind power. In addition, despite of differences in penetration level coefficients of wind power in a MG, the quality of frequency variations was not the same. The best quality of frequency variation in a MG was recorded roughly at 15–20% penetration level.

2. Wind energy conversion system

Wind power generation system is mainly composed of mechanical, electromagnetic, and electrical components. In addition, other components including generator, electric power converter, and power transformers are among the other components of this system. Generally, the configuration of these systems depends upon type of electric machine and their common aspect of power network. From the structural viewpoint, WECS can be either of fixed-speed or variable-speed type. Each of these types, having their own advantages and disadvantages, and each one is used in various applications. One of the important and common components in all WECSs is gearbox located between main shaft of wind turbine and the generator. The essential role of gearbox is to speed up of blades up to the speed of rotor of the generator, i.e. 1000 or 1500 rpm [24,25].

2.1. DFIG-based wind turbine

Figure 1 shows a DFIG-based wind turbine of WECS and two back to back pulse wide modulation (PWM) converters connected to the generator. In this system, wind turbine system is connected to the DFIG through a mechanical shaft system, including a low speed turbine shaft and high-speed generator shaft and an interfaced gearbox. Back to back converter consists of a rotor side convertor and a grid-side one [26,27]. These two converters are connected via a capacitor. Since only part of total power, approximately 25%, is flowing through power electronic converter, thus the size and cost of the converter are reduced meaningfully [28,29]. The need for sliding ring and brush are among the drawbacks of this system, increasing construction and maintenance cost [30]. This type of WECS can potentially reduce the oscillations introduced by wind speed variations. In addition, PWM back to back power electronic converter controls generated power and reaching maximum power point tracking (MPPT) is likely [31,32]. Despite increase in cost as well as power conversion loss, penetration of these types of WECS is constantly growing [33,34].

When speed decreases, the amount of released kinetic energy from wind turbine shafts is ΔF_k which is obtained by Equations (1) and (2).

$$F_k = \frac{1}{2} J\omega_{mech}^2 \tag{1}$$

$$\Delta F_k = F_{k0}\left(1 - \frac{\omega_{mech1}^2}{\omega_{mech0}^2}\right) \tag{2}$$

F_K depends on wind speed varying in the range of zero and unity per unit, ($0\le E_{ko}\le 1.0$pu = f(wind speed)). In addition, ω_{mech1} should not below minimum of circular mechanical speed of a DFIG-based wind turbine ($\omega_{mech\text{-}min}\le\omega_{mech1}$). Moreover, instantaneous power obtained from WT should not exceed maximum allowable power according to the machine data provided by the manufacturer, ($F_{ko}+\Delta F_k\le F_{k,max}$).

Figure 2(a) shows DFIG-based wind turbines controllers trying to maintain turbine in an optimum speed in order to produce maximum power. Operating point power controller obtains $\Delta P_\omega{}^*$ which is based on the measured speed and electrical power. Operating point power is an input to the converter produces torque and power by controlling the generator's rotor currents. Supplemental control signal ($\Delta P_f{}^*$) adopt operating point power in terms of a function of deviation rate of change of network frequency. Supplemental control signal of inertia control ring is proportional to controller parameters (K_{pf}, K_{df}). Initial frequency control occurs when network frequency violates specified limits, activating the added ring. Inserting this signal ($\Delta P_f{}^*$) into torque relation, the torque is adjusted. Once the system frequency drops, operating point torque increases and the speed of rotor is reduced, releasing kinetic energy. The reference point power ($\Delta P_{f\omega}{}^*$) consists of two components: ($\Delta P_f{}^*$) which is based on frequency variation, and ($\Delta P_\omega{}^*$) which is based on the optimum speed if turbine in terms of a function of wind speeds, expressed by Equations (3)–(5) [35]:

$$\Delta P_f^* = -\Delta f\, K_{pf} - \frac{df}{dt} K_{df} \tag{3}$$

$$\Delta P_\omega^* = K_{\omega i}\int(\omega^* - \omega)dt - K_{\omega p}(\omega^* - \omega) \tag{4}$$

$$\Delta P_{f\omega}^{*} = \Delta P_{\omega}^{*} + \Delta P_{f}^{*} \tag{5}$$

K_{df} and K_{pf} are derivative and proportionality gains of controller, respectively. Considering two terms of DFIG's operating point power, $\Delta P_{\omega}{}^{*}$ varies steadily compared to deviation rate of change of operating point power, $\Delta P_{f}{}^{*}$. Thus, when a perturbation is applied at the instant t = 0, $\Delta P_{\omega}{}^{*}$ is considered to be zero. Considering instantaneous variation of operating point power by the converter, it is assumed that $\Delta P_W = \Delta P_{f\omega}{}^{*}$, and Equations (6) and (7) are obtained [18].

$$\Delta P_{f\omega}^{*} = 0 + \Delta P_{f}^{*} \tag{6}$$

$$\Delta P_W = \Delta P_{f\omega}^{*} = \Delta P_{f}^{*} = -\Delta f\, K_{pf} - \frac{df}{dt} K_{df} \tag{7}$$

2.2. DFIG-based WT'S control system model

Figure 2(b) shows, the dynamic model of DFIG against frequency control. The differences between the models given in Figure 2(a,b) is the added reference power based on the frequency variation using wash-out filter with the time constant of Tw. This indicates initial frequency tuning of conventional power production in transient state.

$$\Delta P_{f}^{*} = \frac{1}{R} \Delta X'' \tag{8}$$

In Equation (8), R is the governor droop when wind turbine is used, and $\Delta X''$ is measured frequency variation when wind turbine is connected to the network.

3. Thermal and non-thermal turbines control system model

Dynamic performance of small perturbation of a thermal turbine and a non-thermal are shown in Figure 3. These models consist of parameters such as time constant wind turbine (T_t), constant time without reheat (T_h), and constant time with reheat (T_r) [36,37].

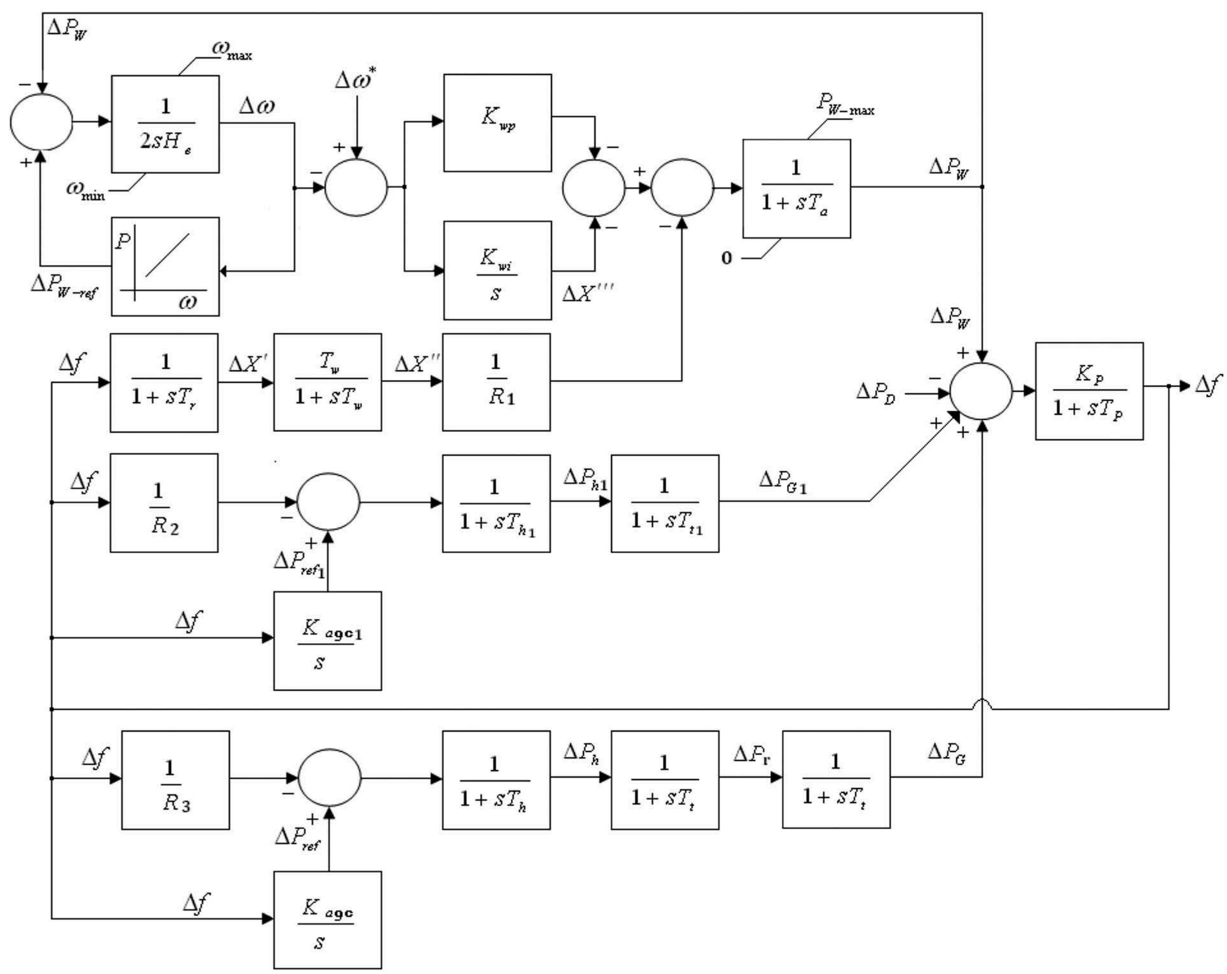

Figure 5. Microgrid dynamic configuration for frequency control.

Table 1. PSO parameters tuning.

PSO	Population	Iteration	ω	c_1	c_2
Parameters	50	20	0.7298	1.4962	1.4962

4. Dynamic model of frequency control of a MG with constant of DFIG-base wind turbine

Figure 4(a) depicts power system diagram, while Figure 4(b) illustrates block diagram of transfer function of a MG compromising of conventional generators and DFIG-based generators for frequency tuning. Equation (9) is obtained by subtraction of load change, ΔP_D, from overall conventional power injections, ΔP_{G1} and ΔP_{G2}, as well as from wind power, ΔP_W, by considering Equation (8).

$$\Delta P_{G1} + \Delta P_{G2} + \Delta P_W - \Delta P_D = \Delta P_f \tag{9}$$

Coefficients T_p and K_p can be seen in Equations (10) and (11) in terms of frequency, damping ratio, and inertia.

$$T_p = \frac{2H}{fD} \tag{10}$$

$$K_p = \frac{1}{D} \tag{11}$$

Based on the model given in Figure 4(b) and considering transfer function of network, load, and generator as $K_P/(1 + T_P s)$ and Equations (7) and (9)–(11), we have:

$$\overbrace{\left(\frac{2H}{f} + K_{df}\right)}^{2H^*} \frac{d\Delta f}{dt} = \Delta P_G + \Delta P_{G1} - \overbrace{\left(K_{pf} + D\right)}^{D^*} \Delta f - \Delta P_D \tag{12}$$

Figure 5 shows the dynamic model of a small perturbation imposed on a MG consisting of the model of thermal turbine, non-thermal turbine and a turbine based on DFIG. This model simulates frequency control model after perturbation and consists of conventional system parameters such as load damping ratio (D), droop (R), inertia (H), and time constants T_t, T_h, and T_r. System behavior depends on the parameters of MG, particularly controller coefficients of WT speed, K_{wi} and K_{wp}. Dynamic model is represented in the steady-state form extended from transfer function of Equation (13).

$$\frac{d\underline{X}}{dt} = A\underline{X} + \Gamma\underline{P} \tag{13}$$

In Equation (13), $\underline{X}$ denotes state vector, $\underline{P}$ denotes perturbation vector, A and Γ denote state and

$$\underline{X} = [\Delta P_{h1}\ \ \Delta P_{ref1}\ \ \Delta P_{G1}\ \ \Delta P_{h2}\ \ \Delta P_{ref2}\ \ \Delta P_r\ \ \Delta P_{G2}\ \ \Delta f\ \ \Delta X'\ \ \Delta X''\ \ \Delta X'''\ \ \Delta\omega\ \ \Delta P_W]^T \tag{14}$$

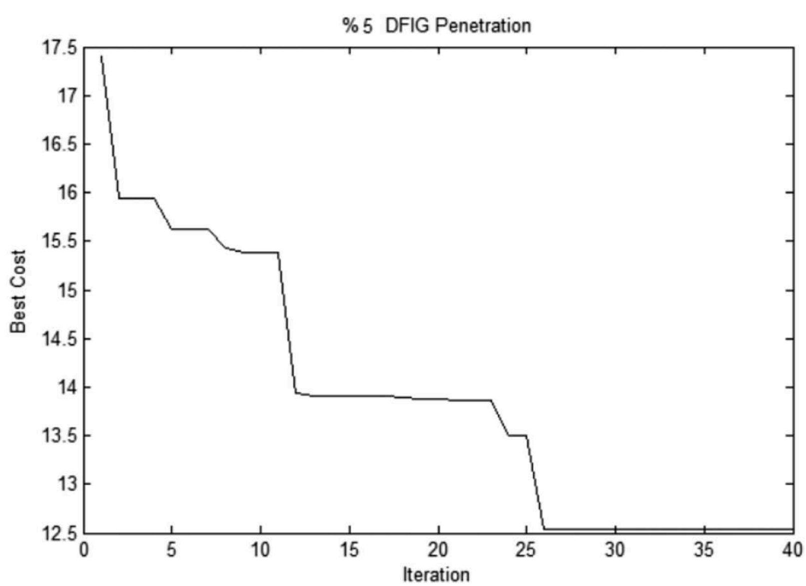

Figure 6. Convergence curve with %5 DFIG penetration (PSO).

perturbation matrix, respectively. State Equation (13) can be extended to Equations (14)–(16).

$$\underline{P} = [0\ 0\ 0\ 0\ 0\ 0\ 0\ \Delta P_D\ 0\ 0\ 0\ 0\ 0]^T \qquad (15)$$

$$\Gamma = \left[0\ 0\ 0\ 0\ 0\ 0\ 0\ \frac{-K_p}{T_p}\ 0\ 0\ 0\ 0\ 0\right]^T \qquad (16)$$

Dynamic simulations are performed while considering various penetration coefficients with/without DFIG in MG and with regard to the load.

5. Optimum tuning of DFIG-based WTS speed controller parameters

PSO is one of the most important swarm-based techniques among the intelligent optimization algorithms. PSO which is also known as bird algorithm is one of the strongest algorithms for optimization of continuous and discrete problems. This algorithm is mostly used for high convergence speed. PSO can be expressed by Newton's mechanical laws. In this algorithm, each particle i with mass of m move throughout D-dimension search space.

Table 2. Optimum DFIG speed controller in different wind penetration.

Wind penetration	%5	%15	%25	%50
Best Cost	6.3693	2.9165	5.8219	13.9137
Settling Time	6.3517	2.9153	5.8181	13.8912
Overshoot	0.0176	0.0012	0.0039	0.0224
K_{wp}	6.5632	7.1054	9.0979	61.3507
K_{wi}	5.2677	0.8851	0.01	0.01

In search for food by birds, it was seen that total data of swarm is used by particles to specify their movements. Thus, the best swarm and individual positions are obtained at any time. New search direction is a combination of these two positions and particle's prior position. In D-dimension search space, the best individual position of particle I and the best swarm position are expressed by: $\vec{p}_i = (p_{i1}, p_{i2}, \ldots, p_{iD})$ and $\vec{g} = (g_1, g_2, \ldots, g_D)$. The position and velocity of each particle i are updated in any iteration by Equations (17) and (18) [38,39].

$$V_i(t+1) = \omega V_i(t) + r_1 c_1 (p_i(t) - x_i(t)) + r_2 c_2 (g_i(t) - x_i(t)) \qquad (17)$$

$$x_i(t+1) = x_i(t) + V_i(t+1) \qquad (18)$$

where ω is inertia coefficient, c1 and c2 are individual and swarm learning coefficients, r1 and r2 are random numbers in [0, 1].

For the simplicity of computation, cost function (Z) is introduced by Equation (19).

$$z = \omega_1 * \text{SettlingTime} + \omega_2 * \text{Overshoot} \qquad (19)$$

where, ω_1 and ω_2 are weighting factors of settling time and maximum overshoot of output frequency in MG, respectively. Both of the weighting factors in cost function are 1. PSO algorithm adjustment for this problem is given in Table 1. Inertia coefficients (ω), individual learning (c_1), and swarm learning (c_2) are available in [40]. Population coefficients and iteration number are obtained empirically by considering problem nature. Figure 6 shows convergence curve of cost function of

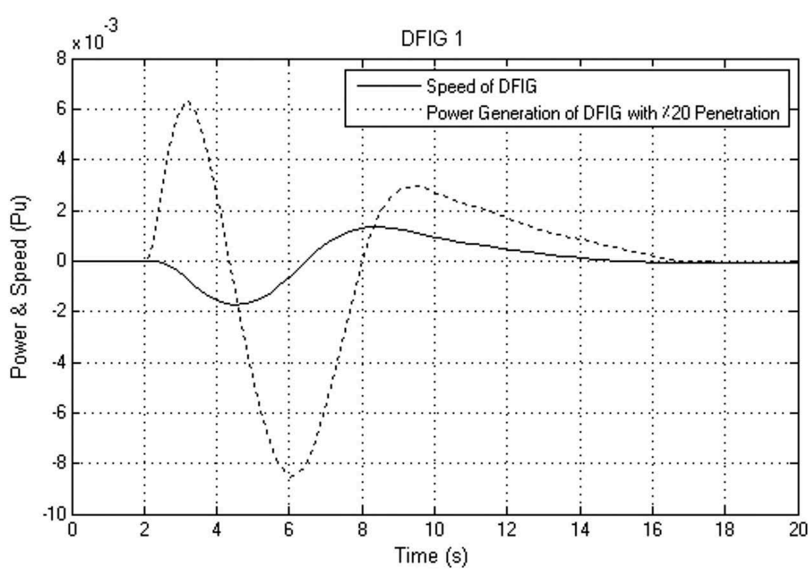

Figure 7. Speed and power variation with %15 DFIG penetration. (a) Speed variation with %5, %10, %15 and %20 DFIG penetration. (b) Power variation with %5, %10, %15 and %20 DFIG penetration.

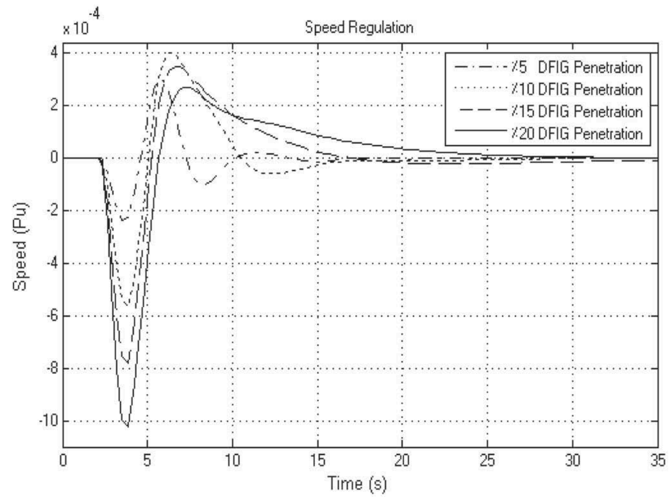

(a) Speed variation with %5, %10, %15 and %20 DFIG penetration

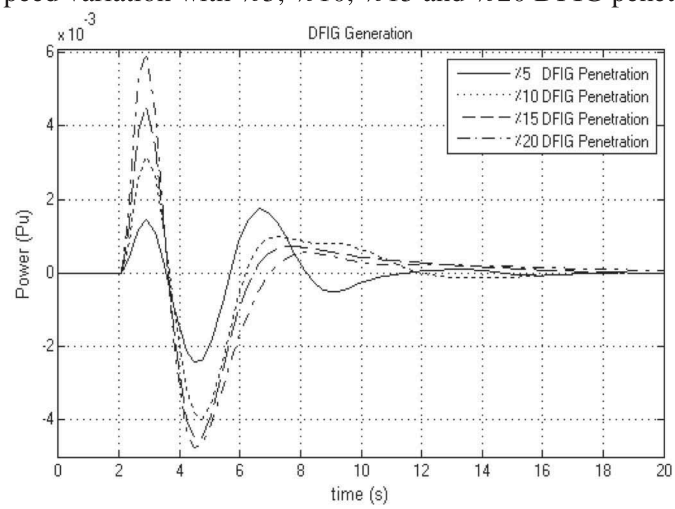

(b) Power variation with %5, %10, %15 and %20 DFIG penetration

Figure 8. Speed and power variation of double-fed induction-generator.

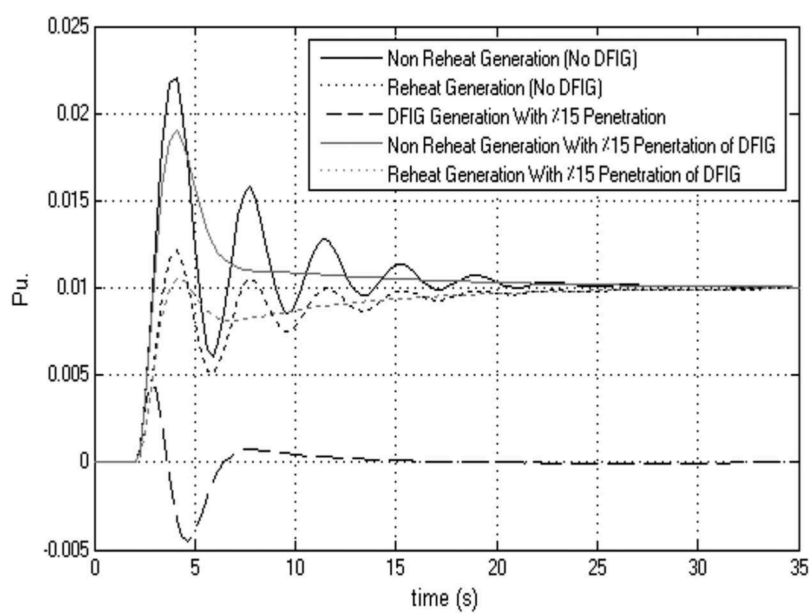

Figure 9. Non-reheat and rehear turbine power generation with %15 DFIG penetration (0.02 Pu disturbance).

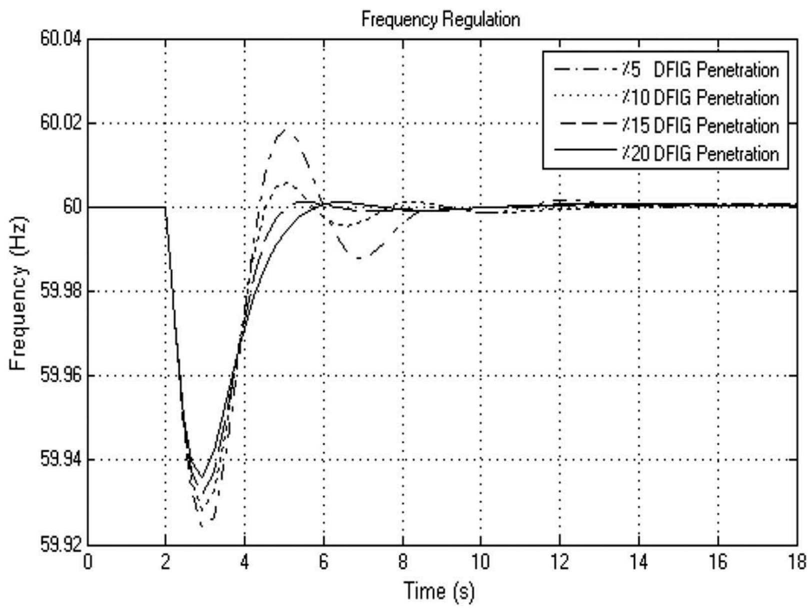

Figure 10. Frequency variation with %5, %10, %15 and %20 DFIG penetration (0.02 Pu disturbance). (a) Frequency variation with %5 DFIG penetration (PSO and ISE) and without DFIG (0.02 Pu disturbance). (b) Frequency variation with %15 DFIG penetration and without DFIG (0.02 Pu disturbance).

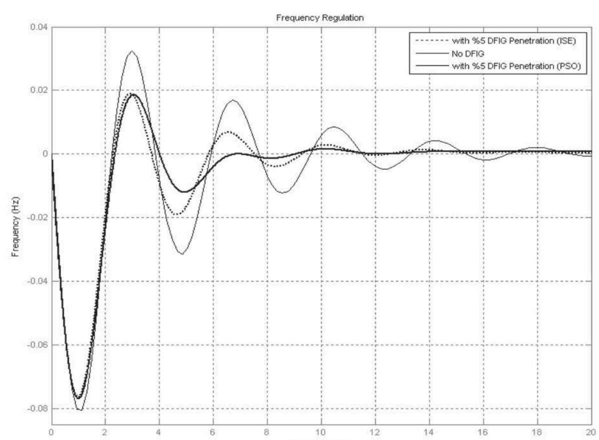

(a) Frequency variation with %5 DFIG penetration (PSO and ISE) and without DFIG (0.02 Pu disturbance)

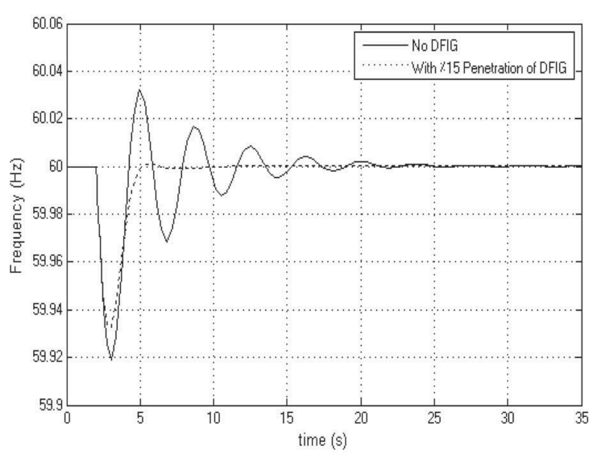

(b) Frequency variation with %15 DFIG penetration and without DFIG (0.02 Pu disturbance)

Figure 11. Frequency variation with 15% and 5% DFIG penetration and without DFIG (0.02 Pu disturbance).

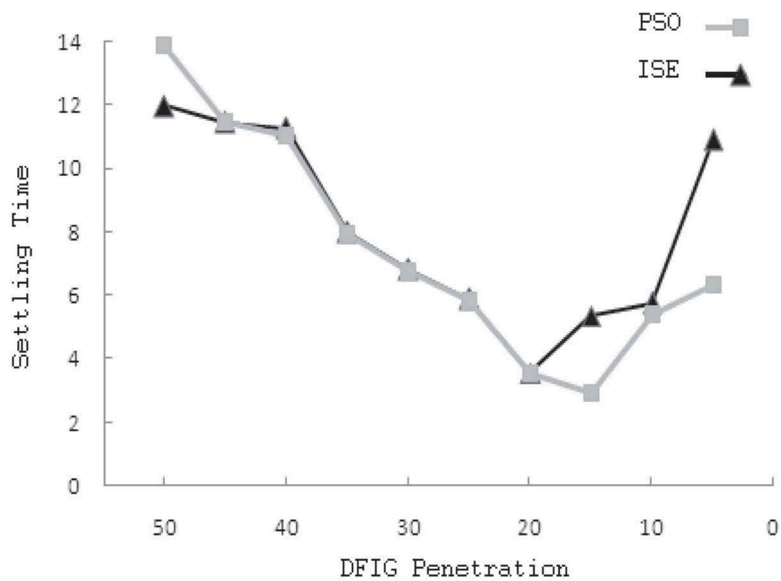

(a) Settling time variation

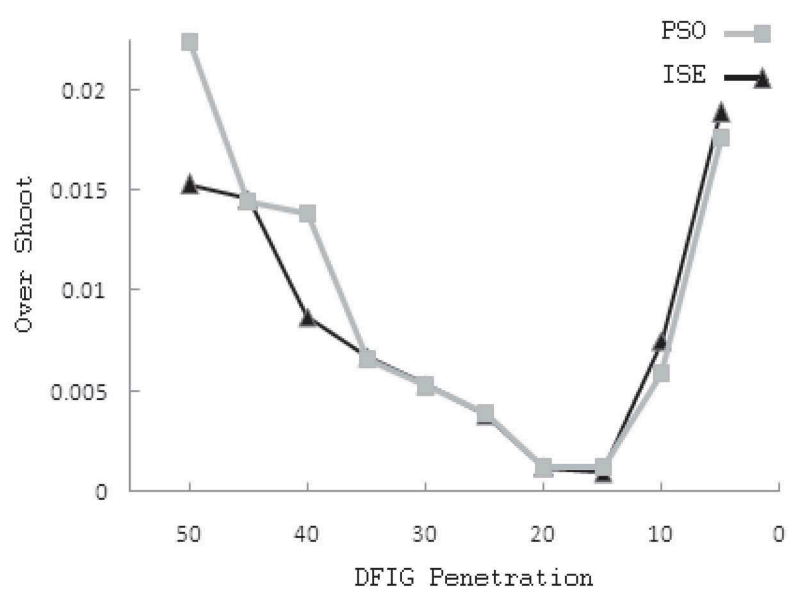

(b) Overshot variation

Figure 12. Settling time and overshot variation in various double-fed induction-generator penetration (0.02 Pu disturbance).

Equation (20) considering 5% wind power penetration in MG. Table 2 presents optimum values of WIND TURBINE's speed controller using PSO and by considering various wind power penetration. In order to evaluate wind power effect on total power supply, penetration index, α_w, is obtained using Equation (20) [18].

$$\alpha_w = \frac{\text{Total Wind Product}}{\text{Total Product from Various source}} * 100 \quad (20)$$

6. Simulation results

Simulations were carried out by considering dynamic model for load increase of 0.02 per unit with and without various penetration coefficients of DFIG-based WTs for the studied MG. In addition, optimal parameters for DFIG-WT's controllers are presented considering results given in Table 2. It should be noted that, supplying extra loads in steady-state are done using conventional generators. Instantaneous load variations and generating power of DFIG are

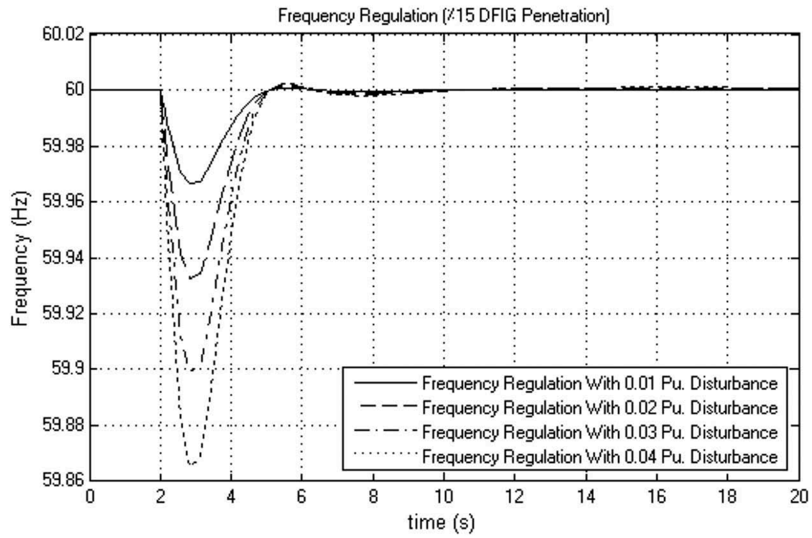

Figure 13. Frequency variation with %15 DFIG penetration (0.01, 0.02, 0.03 and 0.04 Pu disturbance).

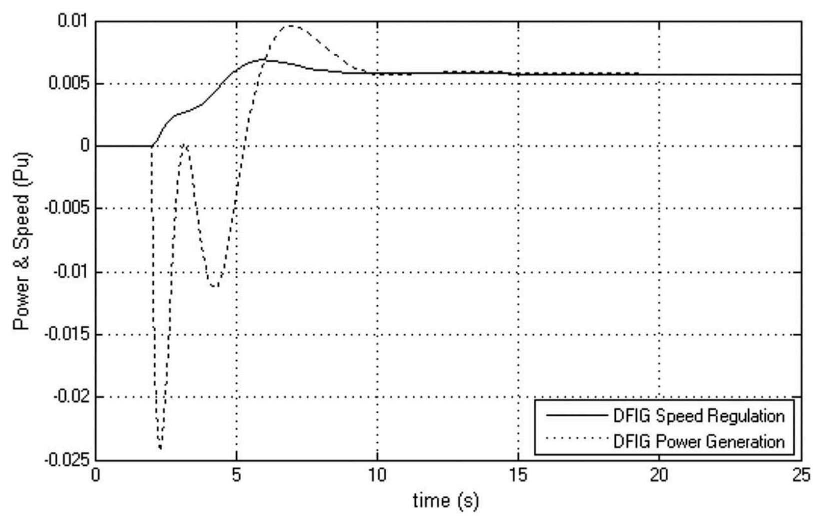

Figure 14. Speed and DFIG power variation with %20 DFIG penetration simultaneous with increase wind speed (0.02 Pu disturbance).

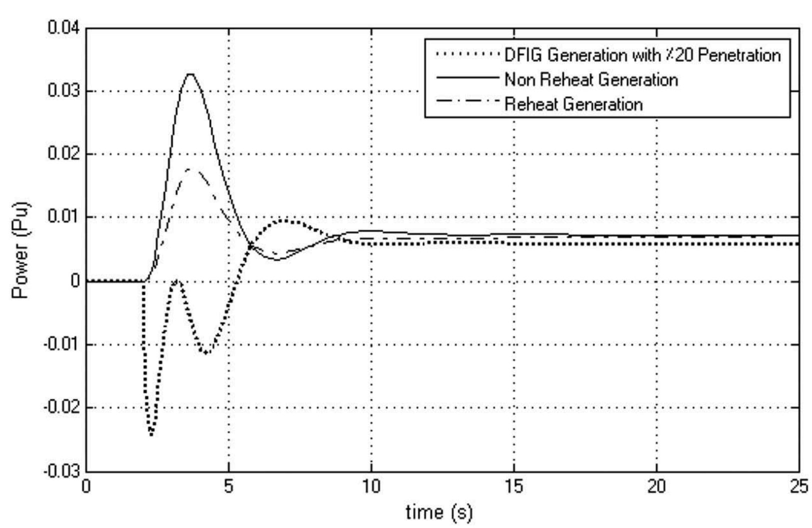

Figure 15. Non reheat and rehear turbine power generation with %20 DFIG penetration simultaneous with increase wind speed (0.02 Pu disturbance).

illustrated in Figures 7 and 8. Generating power changes in conventional generating units in response to the step compensation of load are shown in Figure 9.

In addition, frequency variation of MG in various wind penetration levels is depicted in Figures 10 and 11. It presents a comparison between the proposed method and the ISE method. Figure 7 shows speed change and DFIG generating power at the time of perturbation until reaching stability in wind power penetration level of 15%. According to the figures, once overload is appeared at the instant of 2 sec, DFIG immediately releases kinetic energy by decreasing mechanical energy. Thus, DFIG's output power increases to participate I frequency control. Afterwards, DFIG's output power decreases to fix WT speed at the optimal value. Based on the figure, DFIG's speed controller could retrieve the speed to the appropriate value, and in turn, DFIG's output power returns to the nominal initial value.

Figure 8 show DFIG's speed and output power variations in different wind power penetration levels in MG. Obviously, with the increase of wind power penetration level, the possibility of utilizing released energy by WT blades is also raised. Figure 9 depicts variation of generating units, including thermal, non-thermal, and wind units, in MG. As it is clear, DFIG participates in automatic control of power at the time of perturbation, introduced by overload in transient state in MG, resulting in reduced oscillations of output power of conventional units.

Figures 12 and 13 show the impact of DFIG with various penetration level of wind power in MG on frequency variation. As seen, DFIG could contribute to the improvement of frequency oscillations due to automatic control of power generation. The impact of wind power penetration, in MG, is not the same of all frequency oscillation parameters. Consequently, overshoot and settling time improvements are observed with the steady increase of wind power penetration level up to 15–20%. By contrast, settling time as well as overshoot of frequency variation, in MG, gets raised with penetration level larger than 20%. This, in turn, affects frequency quality. These changes are shown in Figure 1. Also the results of the proposed method is shown in reference [5,19]. It was observed that in the presented method due to the optimal settings for controlling the speed of the wind turbine, the desired computing goals, against Cited references were improved.

Figure 14 shows system response to load variations from 0.01 to 0.04 per unit with penetration coefficient of 15%. It can be seen that the performance of tuning control is effective and the settling time and overshoot amount are greatly improved. The mentioned tuning, therefore, performs appropriately in the small-signal range of load variation, up to 5% variations of total load. Figure 15 shows the effect of wind speed increase on the performance of wind turbine controllers while the turbulence is 0.02 per unit.

7. Conclusion

DFIGs with the capability of power production is produced in different mechanical speeds, By releasing stored mechanical energy in their blades, DFIGs are also able to quickly reduce the speed when the frequency drop occurs, supporting conventional generators in tuning frequency. And this capability is obvious in different penetration level of WTs. The frequency tuning is performed by PSO. It was proved that PSO reach better results in determining optimum values for WT's speed controllers in order to improve important indices of frequency variation compared to the other methods in a MG with conventional generating units. Based on the obtained results, obtaining the best characteristics of frequency variation in a particular penetration level of wind power is feasible in MG. This means less and or more production of energy from WT in a - studied MG, can affect frequency response parameters of MG. Essentially, the increased wind energy will not be advantageous in the MG.

Disclosure statement

No potential conflict of interest was reported by the authors.

References

[1] Huang H, Chung CY. Coordinated damping control design for DFIG-based wind generation considering power output variation. IEEE Trans Power Syst. 2012 Nov;27(4):1916–1925.

[2] Hughes FM, Anaya-Lara O, Jenkinas N, et al. A power system stabilizer for DFIG-base wind generation. IEEE Trans Power Syst. 2006 May;21(2):763–772.

[3] Ko W, Hur D, Park JK. Correction of wind power forecasting by considering wind speed forecast error. J Int Council Electr Eng. 2015 Aug;5(1):47–50.

[4] Jafari A, Shahgholian G. Analysis and simulation of a sliding mode controller for mechanical part of a doubly-fed induction generator based wind turbine. IET Gener Transm Distrib. 2017 Jul;11(10):2677–2688.

[5] Cheng F, Qu L, Qiao W. Fault prognosis and remaining useful life prediction of wind turbine gearboxes using current signal analysis. IEEE Trans Sustain Energy. 2018 Jan;9(1):157–167.

[6] Beik O, Schofield N. High-voltage hybrid generator and conversion system for wind turbine applications. IEEE Trans Industr Electron. 2018 Apr;65(4):3220–3229.

[7] Jalali M, Bhattacharya K. Frequency regulation and AGC in isolated systems with DFIG based wind turbines. Proceeding of the IEEE/PES; 2013 Jul; Vancouver, BC. p. 1–5. DOI:10.1109/PESMG.2013.6672801

[8] Park G, Kim J, Kang YC. Transient voltage control of a DFIG-basedwind power plant for suppressing overvoltage using a reactive current reduction loop. J Int Council Electr Eng. 2016 Jun;6(1):140–145.

[9] Hosseini E, Shahgholian G. Partial- or full-power production in WECS: a survey of control and structural strategies. Eur Power Electron Drives. 2017 Dec;27(3):125–142.

[10] Rahimi M. Improvement of energy conversion efficiency and damping of wind turbine response in grid connected DFIG based wind turbines. Int J Electr Power Energy Syst. 2018 Feb;95:11–25.

[11] Yang B, Jiang L, Wang L, et al. Nonlinear maximum power point tracking control and modal analysis of DFIG based wind turbine. Int J Electr Power Energy Syst. 2016 Jan;74:429–436.

[12] Ko HS, Yoon GG, Kyung NH, et al. Modeling and control of DFIG-based variable-speed wind-turbine. Electr Power Syst Res. 2008 Nov;78(11):1841–1849.

[13] Attya AB, Hartkopf T. Penetration impact of wind farms equipped with frequency variations ride through algorithm on power system frequency response. Int J Electr Power Energy Syst. 2012 Sep;40(1):94–103.

[14] Rohilla V, Parmar KPS, Saini S. Optimization of AGC parameters in the restructured power system environment using GA. Int J Eng Sci Emerging Technol. 2012 Oct;3(2):30–40.

[15] Liao Y, Li H, Yao J, et al. Operation and control of a grid-connected DFIG-based wind turbine with series grid-side converter during network unbalance. Electr Power Syst Res. 2011 Jan;81(1):228–236.

[16] Rabelo BC, Hofmann W, Silva JLD, et al. Reactive power control design in doubly fed induction generators for wind turbines. IEEE Trans Industr Electron. 2009 Oct;56(10):4154–4162.

[17] Motamed B. The effect of high penetration of wind power on primary frequency control of power systems. Goteborg: Chalmers University of Technology; 2013.

[18] Mauricio JM, Marano A, Eeposito AG, et al. Frequency regulation contribution through variable speed wind energy conversion system. IEEE Trans Power Syst. 2009 Feb;24(1):173–180.

[19] Bhatt P, Ghoshal SP, Roy R. Load frequency stabilization by coordinated control of thyristor controlled phase shifters and superconducting magnetic energy storage for three types of interconnected two area power systems. Electr Power Energy Syst. 2010;32:1111–1124.

[20] Talaq J, Basri FA. Adaptive fuzzy gain scheduling for load frequency control. IEEE Trans Power Syst. 1999 Feb;14(1):145–150.

[21] Padhan D, Majhi S. A new control scheme for PID load frequency controller of single area and multi area power system. ISA Trans. 2013;52:242–251.

[22] Manikandan N, Karthikeyan G. Fuzzy based load frequency control in an interconnected power system with wind turbine. J Innovative Res Solution. 2013 Jan;1(2):71–79.

[23] Verma YP, Kumar A. Load frequency control in deregulated power system with wind integrated system using fuzzy controller. Front Energy. 2013;7(2):245–254.

[24] Luna A, Lima FKA, Santos D, et al. Simplified modeling of a DFIG for transient studies in wind power applications. IEEE Trans Industr Electron. 2011 Jan;58(1):9–20.

[25] Jain B, Jain S, Nema RK. Control strategies of grid interfaced wind energy conversion system: an overview. Renew Sust Energ Rev. 2015 Jul;47: 983–996.

[26] Lei T, Barnes M, Ozakturk M. Doubly-fed induction generator wind turbine modelling for detailed electromagnetic system studies. IET Renewable Power Gener. 2013 Mar;7(2):180–189.

[27] Chena Q, Lib Y, Seemc JE. Dual-loop self-optimizing robust control of wind power generation with doubly-fed induction generator. ISA Trans. 2015 Sep;58:409–420.

[28] Smith AC, Todd R, Barnes M, et al. Improved energy conversion for doubly fed wind generators. IEEE Trans Ind Appl. 2006 Nov–Dec;42(6):1421–1428.

[29] Gao L, Guan B, Zhou Y, et al. Model reference adaptive system observer based sensorless control of doubly fed induction machine. Proceeding of the IEEE/ ICEMS; 2010 Oct; Incheon, South Korea. p. 931–936.

[30] Mahdavian M, Wattanapongsakorn N, Shahgholian G, et al. Maximum power point tracking in wind energy conversion systems using tracking control system based on fuzzy controller. Proceeding of the IEEE/ ECTICON; 2014; Nakhon Ratchasima. DOI:10.1109/ ECTICon.2014.6839750

[31] Petersson A, Harnefors L, Thiringer T. Evaluation of current control methods for wind turbines using doubly fed induction machine. IEEE Trans Power Electron. 2005 Jan;20(1):227–235.

[32] Haque ME, Negnevitsky M, Muttaqi KM. A novel control strategy for a variable speed wind turbine with a permanent magnet synchronous generator. IEEE Trans Ind Appl. 2010 Jan–Feb;46(1): 331–339.

[33] Shahgholian G, Khani K, Moazzami M. The Impact of DFIG based wind turbines in power system load frequency control with hydro turbine. J Iranian Dam Hydroelectric. 2015 Winter;1(3):38–51.

[34] Mozafarpoor-Khoshrodi SH, Shahgholian G. Improvement of perturb and observe method for maximum power point tracking in wind energy conversion system using fuzzy controller. Energy Equip Syst. 2016 Autumn;4(2):111–122.

[35] Morren J, de Haan SWH, Kling WL, et al. Wind turbines emulating inertia and supporting primary frequency control. IEEE Trans Power Syst. 2006 Feb;21(1):433–434.

[36] Debbarma S, Saikia LC, Sinha N. Solution to automatic generation control problem using firefly algorithm optimized $I^{\lambda}D^{\mu}$ controller. ISA Trans. 2014 Mar;53 (2):358–366.

[37] Yua HY, Bansalb RC, Donga ZY. Fast computation of the maximum wind penetration based on frequency response in small isolated power systems. Appl Energy. 2014 Jan;113:648–659.
[38] Pain S, Acharjee P. Multi objective optimization of load frequency control using PSO. Int J Emerging Technol Adv Eng. 2014 Apr;4(7):16–22.
[39] Jaber AS, Ahmad AZ, Abdalla AN. An investigation of scaled FLC using PSO for multi area power system load frequency control. Energy Power Eng. 2013;5 (4):458–462.
[40] Eberhart RC, Shi Y. Particle swarm optimization: developments, applications and resources. IEEE Proc Congr Evol Comput. 2001;1:81–86.